

Active and Passive Properties of Rabbit Descending Colon: A Microelectrode and Nystatin Study

N.K. Wills*, S.A. Lewis, and D.C. Eaton**

Department of Physiology, Yale University School of Medicine, 333 Cedar Street,
New Haven, Connecticut 06510

Received 25 April 1978; revised 31 July 1978

Summary. The electrical properties of the basolateral membrane of rabbit descending colon were studied with microelectrode methods in conjunction with the polyene antibiotic nystatin. Two problems were examined: (i) the relative distribution of tight junctional, apical membrane and basolateral membrane resistances, and (ii) the ionic basis of the basolateral membrane potential. Intracellular K^+ activity (K^+) was measured using liquid ion exchanger microelectrodes ($(K^+) = 76 \pm 2$ mM) and was found not to be in equilibrium with the basolateral membrane potential. In order to measure membrane resistances and to estimate the selective permeability of the basolateral membrane, the apical membrane was treated with nystatin and bathed with a K_2SO_4 Ringer's solution which was designed to mimic intracellular K^+ composition. This procedure virtually eliminated the resistance and electromotive force of the apical membrane. Shunt resistance was calculated by two independent methods based on microelectrode and transepithelial measurements. Both methods produced similar results ($R_s = 691 \pm 63 \Omega \text{ cm}^2$ and $770 \pm 247 \Omega \text{ cm}^2$, respectively). These findings indicate that the shunt has no significant selectivity, contrary to previous reports. Native apical membrane resistance was estimated as $705 \pm 123 \text{ V cm}^2$ and basolateral membrane resistance was $95 \pm 14 \text{ V cm}^2$.

To estimate basolateral membrane selectivity, the serosa was bathed in a NaCl Ringer's solution followed by a series of changes in which all or part of the Na^+ was replaced by equimolar amounts of K^+ . From measures of bi-ionic potentials and conductance during these replacements, we calculated potassium permeability and selectivity ratios for the nystatin-treated colon by fitting these results to the constant field equations. By correcting for shunt conductance, it was then possible to estimate the selective permeability of the basolateral membrane alone. Selectivity estimates were as follows: $P_{Na}/P_K = .08$ and $P_{Cl}/P_K = .07$ (uncorrected for shunt) and $P_{Na}/P_K = .04$ and $P_{Cl}/P_K = .06$ (basolateral membrane alone).

In a second set of experiments, evidence for an electrogenic Na^+ pump in the basolateral membrane is presented. A small ouabain-sensitive potential could be generated in the nystatin-treated colon in the absence of chemical or electrical gradients by mucosal, but not serosal, addition of NaCl. We conclude that this electrogenic pump may contrib-

* To whom reprint requests should be made.

** Present address: Department of Physiology and Biophysics, University of Texas Medical Branch, Galveston, Texas 75550.

ute to the basolateral membrane potential; however, the primary source of this potential is "passive": specifically, a potassium gradient which is maintained by an "active" transport process.

An appendix compares the results of nystatin experiments to amiloride experiments which were conducted separately on the same tissues. The purpose of this comparison was to develop a comprehensive model of colonic transport. The analysis reveals a leak conductance in the apical membrane and the presence of an amiloride-insensitive conductance pathway.

Present research in epithelial transport has shown an upsurge in the use of antibiotic and ionophoretic agents (Frizzell 1977; Frizzell & Turnheim, 1978; Reuss, 1978). Recently Lewis *et al.*, (1977) demonstrated the usefulness of the polyene antibiotic nystatin as a tool for investigating the electrical properties of the mammalian tight epithelium, rabbit urinary bladder. Lewis *et al.* found that when nystatin was added to the mucosal bathing solution, short-circuit current was significantly increased and transepithelial resistance was greatly reduced. These results were caused by an increase in apical membrane conductance, primarily to Na^+ and K^+ . A slight increase in permeability was also induced for Cl^- , although this increase was smaller than that observed for cations. $P_{\text{Cl}}/P_{\text{K}}$ for nystatin-induced permeability was estimated as 0.28. Larger cations (e.g., choline) showed no significant increase in permeability.

Previous studies of nystatin on biological and artificial membranes indicated that this drug produces small aqueous channels, approximately 8 Å in diameter (Holz & Finkelstein, 1970; Cass & Dalmark, 1973). The relatively small size of the channels permit penetration of the membrane by small monovalent ions such as Na^+ , K^+ and Cl^- ; however, divalent ions or ions larger than glucose are impermeable (Cass, Finkelstein & Krespi, 1970). Thus Lewis *et al.* (1977) concluded that the action of nystatin on the apical membrane of rabbit urinary bladder was similar to that observed on other biological membranes.

The effects of nystatin in most biological tissues are reversible by washing the cells with an appropriate nystatin-free medium. Consequently, nystatin affords a distinct experimental advantage as it permits the investigator to alter the electrolyte composition of cells in a reversible, nondetrimental fashion without significantly altering other intracellular constituents (Cass & Dalmark, 1973; Russell, Eaton & Brodwick, 1977).

The present study examines the action of nystatin on a second mammalian epithelium, rabbit descending colon. We report conventional and ion-specific microelectrode measurements which indicate that nystatin has a similar action on both colon and urinary bladder. The aims of the study are twofold: (i) to resolve the electrical resistance of the colon into junctional, basolateral, and apical membrane components (R_j , R_b , and R_a , respectively), and (ii) to determine the ionic basis and mechanism of the basolateral membrane potential in this tissue. To achieve the second aim, we use nystatin to create a preparation which electrically represented the basolateral membrane in parallel with a paracellular shunt pathway. We then assess the selectivity of the basolateral membrane and examine the activity of an electrogenic pump. In an appendix, the results of amiloride and

nystatin experiments that were conducted sequentially on the same tissues are compared and a comprehensive equivalent circuit model of the colon is proposed.

Materials and Methods

With the exceptions noted below, procedures and electrical measurements followed those of Lewis, Wills and Eaton (1978).

Preparation

Male adult New Zealand white rabbits were sacrificed with an injection of sodium pentobarbital (Nembutal), and a section of the descending colon was removed. The underlying muscle layers were removed by blunt dissection (Frizzell, Koch & Schultz, 1976). The dissected tissue was gently mounted on a silicone-greased Delrin ring and positioned between modified Ussing chambers which were designed to: (i) eliminate edge damage, (ii) easily accommodate microelectrode impalements, (iii) reduce hydrostatic gradients, and (iv) allow impalements while stirring and gassing the serosal solution (for further description, see Lewis, 1977).

Electrical Measures

Transepithelial voltage (V_T) was measured with 100 mM LiCl agar bridges placed 5 mm from each side of the tissue and referenced to the serosal solution. Ag-AgCl electrodes placed at opposite ends of the chambers were used to deliver current pulses and to monitor short-circuit current (I_{sc}). Voltage and current electrodes were led to an automatic voltage clamp. V_T , I_{sc} and the microelectrode reading (V_{bi}) were displayed on Analogic digital voltmeters and single channels of a paper chart recorder. In addition, all signals were interfaced on line with a laboratory computer (Digital Equipment, Inc.). Voltages were measured within ± 0.1 mV and were corrected for junction potentials arising from the LiCl bridges or asymmetrical solutions.

Series Resistance—Corrections: Series resistance was measured from the voltage response to a square current pulse applied across the tissue. As shown in Fig. 1B, the voltage deflection V_s produced by the series resistance (R_{series}) is instantaneous, whereas V_T is time dependent. The time dependence of V_T is a property of the parallel combination of the tissue capacitance (C_T) and resistance (R_T) (shown in Fig. 1A). Series resistance was calculated by dividing the instantaneous voltage deflection (V_s) by the magnitude of the current pulse (I) using Ohm's Law, $V_s/I = R_{series}$ (see Fig. 1B). The average series resistance corrected for the area of our chamber opening (2 cm^2) was $60 \Omega \text{ cm}^2$. Since series resistance constituted over 10% of the total resistance, all measurements of transepithelial resistance were corrected for this component.

Because R_{series} equals the sum of mucosal chamber and serosal chamber series resistance ($R_{series} = R_{se} + R'_{se}$), the distribution of series resistance in each chamber was also measured using microelectrodes (see Fig. 1A). In all, a uniform distribution was observed ($R_{se} = R'_{se}$). Voltage divider ratios (α) were also corrected for series resistance.

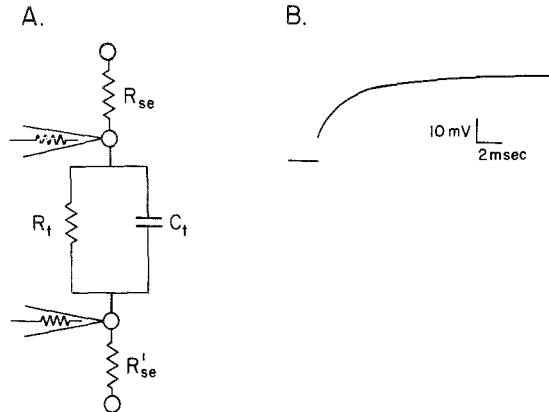


Fig. 1. Summary of method for measuring series resistance. (A): Simplified equivalent circuit representing total series resistance (R_{series}) as two resistors (R_{se} and R'_{se}) placed in series on each side of the preparation (R_T = transepithelial resistance and C_T = tissue capacitance). R_{se} and R'_{se} were measured by microelectrodes positioned next to the apical and basolateral membranes. (B): Tracing of an oscilloscope record of the transepithelial voltage response to a square-wave current pulse (I). R_{series} was calculated from the instantaneous voltage deflection (V_s) indicated by the discontinuous portion of the trace, and Ohm's Law ($V_s/I = R_{\text{series}}$). Note that the remainder of the voltage response is time dependent due to tissue capacitance

Microelectrodes

Conventional Microelectrodes: Microelectrodes were pulled from fiber-filled Pyrex glass tubing and filled with 3 M KCl solution (tip resistance ± 20 -80 M Ω). A WPI (model 750) electrometer measured microelectrode potentials, and fine positioning of the microelectrodes was achieved with a hydraulic microdrive (Stoelting). All microelectrode impalements were from the mucosal side of the tissue and referenced to the serosal solution.

K⁺-Sensitive Microelectrodes: Construction of K⁺ liquid ion exchanger microelectrodes was identical to that described by Lewis, Wills and Eaton (1978). Because of the relatively high resistance of these microelectrodes (10^8 - 10^{10} Ω), potentials were measured with a high input impedance operational amplifier (Teledyne Philbrick 1035). Intracellular potassium activity (a'_K) was calculated from the following equation (Russell *et al.*, 1977):

$$a'_K = (a_K^o + K_{K/Na} a_{Na}^o) \left[\exp \frac{nF}{RT} (V_i - V_o - V_{bl}) \right] \quad (1)$$

where a_K is extracellular potassium activity, $K_{K/Na}$ is the microelectrode selectivity for potassium over sodium, a_{Na}^o is extracellular sodium, V_{bl} is the basolateral potential, V_i is the microelectrode reading inside the cell, n is the correction factor for nonideal slopes, V_o is the microelectrode reading in the outside solution (arbitrarily set to zero), and F , R , and T have their usual meanings.

Throughout this paper brackets [] will be used to denote concentration and parentheses () will mean activity.

Criteria for Successful Impalement: A critical and obvious factor for reliable microelectrode measurements is to avoid significant amounts of membrane damage. As previously reported by our laboratory (Lewis *et al.* 1977), nystatin techniques provide a convenient means for identifying impalement damage. Normally a linear relationship should exist between the transepithelial conductance (G_T) and the voltage divider ratio ($\alpha \equiv R_a/R_{bi}$) as R_a is decreased by nystatin (*see* Eq. (2), below). However, in the presence of membrane impalement damage, the initial value of α will be artifactually low because of a large shunt conductance in the apical membrane. Thus, the relationship between G_T and α will be nonlinear at low values of α . Impalements which demonstrated this type of nonlinear behavior were excluded from data analysis.

A second concern was that leakage of KCl from the microelectrode tip might alter intracellular ion composition. Indeed, we have observed some instances of a gradual and continuous hyperpolarization of V_{bi} without a concomitant increase in the voltage divider ratio. In a few cases these increases exceeded the initial values by 20-30 mV. Consequently, two additional criteria were used to define a successful impalement. These were: (i) that the potential must achieve a steady-state value in less than 1 sec and must remain stable for the duration of measurements in this cell and (ii) that the voltage divider ratio must also remain constant (unless otherwise altered with nystatin or amiloride).

Solutions

The composition of the bathing solutions is given in Table 1. All solutions were gassed with 95% O₂ and 5% CO₂ and maintained at a pH of 7.4 and a temperature of 37°C. Nystatin (Sigma) was dissolved in methanol at a concentration of 5 mg/ml (88,000 units/ml) and was added in microliter aliquots to the mucosal solution. Amiloride (a generous gift of Merck, Sharp and Dohme) and ouabain (Sigma) were dissolved in NaCl and K₂SO₄ Ringer's solutions.

The serosa was normally bathed with NaCl Ringer's and the mucosal bathing solution was potassium sulfate Ringer's. There were two reasons for this choice: First, we wished to mimic intracellular potassium composition across the apical membrane for the purposes of the selective permeability studies. Second, we have found that use of potassium sulfate mucosal solutions greatly increases the viability of the nystatin-treated tissue. Addition of nystatin to NaCl Ringer's causes the preparation to rapidly deteriorate (V_T and R_T decline within 20 min), presumably due to cell swelling and desquamation. To design the potassium solution, we used a K⁺ activity which matched intracellular K⁺ activity as measured with ion-sensitive microelectrodes (*see* below). Sulfate was used instead of Cl⁻ to mimic impermeable intracellular ions since Cl⁻ is known to be permeable through nystatin channels (Lewis *et al.*, 1977). This procedure resulted in viable nystatin-treated tissues which could be maintained for 1-3 hr with stable values of R_T and V_T .

The following results are expressed as the mean \pm SEM based on the number of tissues studied. Differences between means were analyzed using the *t* test for paired or independent means where appropriate.

Results

In this section we first report the effect of apically applied nystatin on the electrical properties of the rabbit descending colon, and then demonstrate that the

Table 1. Composition of bathing solutions (in mM)

Solution	Na	K	Cl ⁻	Ca ²⁺	Mg ²⁺	HCO ₃ ⁻	H ₂ PO ₄ ⁻	SO ₄ ²⁻	MeSO ₃ ⁻	Sucrose	Glucose
NaCl Ringer's	136.2	7	121	2	1.2	25	1.2	1.2	0	0	11.1
KCl Ringer's	0	143.2	121	2	1.2	25	1.2	1.2	0	0	11.1
Na ₂ SO ₄	136	7	0	10	1.2	25	1.2	59	20	120	11.1
K ₂ SO ₄	0	143	0	10	1.2	25	1.2	59	20	120	11.1

nystatin response allows the calculation of the individual resistive properties of the colon. We next present two experiments designed to identify the ionic basis of the basolateral membrane potential.

The Electrical Effects of Nystatin

In general, the effects of nystatin on the electrical properties of the colon were identical to its effects on rabbit urinary bladder. A summary of the results is given in Table 2. The addition of nystatin (120 unit/ml) to the mucosal bathing solution (K_2SO_4 Ringer's, *see Methods*) evoked a rapid hyperpolarization of the transepithelial potential ($\Delta V_T = 27$ mV), a decrease in the voltage divider ratio ($\alpha \cong 0$), and an increase in transepithelial conductance ($G_T = 11$ mmhos/cm²). The basolateral membrane potential simultaneously depolarized slightly ($\Delta V_{bl} = 3$ mV). In all cases, the increase in G_T was linearly related to the decrease in α . (This relationship will be described in more detail below.) The rate of response to nystatin was fastest when the solution was stirred and slowest in the presence of mucous on the apical surface. Under optimal conditions, full effects occurred within 120 sec. The effects could be completely reversed within the first hour of nystatin treatment by washing the mucosa with potassium sulfate Ringer's solution.

I. Membrane and shunt resistance values estimated from microelectrode experiments. Table 2 also presents estimated resistances for the shunt and for the apical and basolateral membranes. To calculate these values, we used an equivalent circuit analysis based on a simple equivalent circuit of the nystatin-treated colon shown in Fig. 2. We will initially consider only the resistance properties of this circuit, specifically transepithelial conductance ($G_T = 1/R_T$) and a voltage divider term which we will define as $(1 + \alpha)^{-1}$. If nystatin nonselectively increases cation conductance in the apical membrane (indicated by the variable resistor in Fig. 2), then a linear relationship can be derived as follows:

$$G_T = (1 + \alpha)^{-1}G_{bl} + G_s \quad (2)$$

where G_s is shunt conductance (nominally assumed to be tight junctional conductance) and G_{bl} is basolateral membrane conductance (Lewis *et al.*, 1977). Thus the magnitude of the shunt conductance can be estimated from the zero G_T intercept of this function and G_{bl} can be calculated from the slope. A typical experimental result is shown in Fig. 3a. As can be seen in this example, the relationship between G_T and $(1 + \alpha)^{-1}$ was linear, as would be expected if only the conductance of the apical membrane was increased. Furthermore, the voltage divider ratio was decreased to approximately zero and remained constant after nystatin treatment. These results indicate that the effects of nystatin are localized to the apical membrane, similar to its action on rabbit urinary bladder.

Using Eq. (2), we calculated mean values for $R_s(1/G_s)$, $R_{bl}(1/G_{bl})$ and $R_a(\alpha R_{bl})$ from six microelectrode experiments (*see Table 2*). It must be noted that these resistance estimates are normalized to 1 cm² of chamber opening and therefore must be corrected for actual membrane area.

II. Shunt resistance and E_{bl} estimated from transepithelial measurements. Employing an analysis similar to Yonath and Civan (1971), we can estimate shunt

Table 2. Nystatin microelectrode results

	V_T (mV)	R_T (Ωcm^2)	V_{bl} (mV)	α	Estimated resistance (Ωcm^2)		
					R_a	R_{bl}	R_s
Control (K_2SO_4 mucosal solution, NaCl serosal solution)	-20 ± 5	386 ± 49	-52 ± 1	8 ± 1	705 ± 123	95 ± 14	691 ± 63
Nystatin (120 units/ml mucosal solution) $n = 6$	-47 ± 1^c	91 ± 13^b	-49 ± 2^a	$\sim 0^a$	~ 0	---	---

^a $P < .05$.^b $P < .01$.^c $P < .001$.

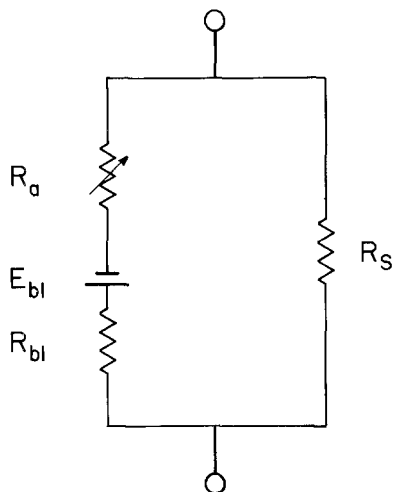


Fig. 2. Equivalent circuit for nystatin experimental conditions. Apical membrane resistance (R_a) is nonselectively decreased by nystatin. E_a^{Na} has been reduced to approximately zero and therefore has been eliminated from the circuit. R_{bl} and E_{bl} are the resistance and emf of the basolateral membrane. R_s is shunt resistance. For description, see text

resistance using transepithelial measurements. This analysis is also based on the equivalent circuit presented in Fig. 2, except that we now include the effects of possible circuit batteries. The validity of the transepithelial estimate of R_s depends on the assumption that no significant batteries are present at the apical membrane or tight junctions. Because the apical membrane is bathed with a solution which is designed to mimic intracellular K^+ composition, we believe it is reasonable to assert that no significant batteries remain at this membrane. (Further evidence for this point will be presented below.)

In contrast, the assertion that no significant battery is present at the tight junction requires further support since Frizzell *et al.* (1976) have postulated a potassium selective paracellular pathway in rabbit colon. One might ask what effect such a paracellular emf would have on our resistance and potential measurements. One reasonable expectation would be that in untreated colon a tight junctional diffusion potential should be generated when the tissue is bathed in asymmetrical potassium solutions. Assuming the P_{Na}/P_K value for the junction reported by Frizzell *et al.*, we calculate that a transepithelial potential of approximately -53 mV should occur when the mucosal NaCl bathing solution is replaced by KCl Ringer's solution (and the serosa is bathed with our normal NaCl Ringer's solution). However, we have performed this procedure and find no significant increase in V_T . In general ΔV_T is less than -10 mV. Therefore, the presence of such potassium selectivity in the junctions is suspect on the basis of transepithelial voltage measurements.

Stronger evidence against potassium selectivity in the shunt pathway comes from the possible effects of such an emf on shunt resistance estimates. Our previous microelectrode estimate of R_s is independent of junctional batteries (see Eq.

(2) above), however, as will be shown below, transepithelial estimates of R_s will be affected by this battery. According to the circuit, G_T should be a linear function of short-circuit current (I_{sc}) as follows:

$$G_T = (E_{bl})^{-1}(I_{sc}) + G_s \quad (3)$$

where E_{bl} is the emf of the basolateral membrane. Any tight junctional emf in the circuit would be lumped into the shunt conductance term. Thus this "transepithelial" value for G_s will be larger or smaller than a "microelectrode" estimate of G_s (see Eq. (2)), depending on the orientation of the shunt battery.

An example of a "transepithelial" estimate of G_s is shown in Fig. 3b. As predicted by Eq. (3), the relationship between G_T and I_{sc} was linear. The mean value ($n = 6$) of G_s calculated in this manner was $1.30 \pm .004$ mmhos. This value was not statistically different from the "microelectrode" G_s estimate ($G_s = 1.43 \pm .001$ mmhos; t test for paired means = .53; $df = 5$). We believe that the agreement of these two estimates strongly indicates that no significant battery is present at the tight junctions during these experiments. Therefore, in the following permeability studies, the shunt is treated as a simple nonselective pathway.

In addition to calculating G_s , it was also possible to estimate the magnitude of the basolateral membrane emf from the transepithelial analysis described above (Eq. (3)). The average estimate of E_{bl} from 6 experiments was -57 ± 3 mV. This estimate is in good agreement with the measured value for V_{bl} (-52 ± 1 mV) for these experiments. The estimate is also in agreement with Schultz, Frizzell and Nellans (1977) who estimated the basolateral membrane emf at -53 mV. The similarity of these estimates provides further support for our assertion that no significant batteries were present at the apical membrane during the nystatin experiments, as this value would have been reflected in E_{bl} .

Properties of the Basolateral Membrane

To identify the ionic bases of the basolateral membrane potential, three experiments were performed. First, we measured the intracellular K^+ activity to determine if K^+ is in electrochemical equilibrium across the basolateral membrane. Next, the relative selective permeability of the basolateral membrane was assessed, and lastly, the presence of an electrogenic pump was determined.

I. Intracellular K^+ Activity. Intracellular K^+ activities were measured with single-barreled ion-sensitive microelectrodes. To avoid the possibility of membrane damage artifacts, the measured α for conventional microelectrodes was compared to the measured α for K^+ -selective microelectrodes. The K^+ activity was calculated from data where the two α 's were not significantly different. Activity values were calculated according to Eq. (1) (see *Methods*) with V_o equal to zero for all impalements. During these experiments the colon was bathed on both sides with NaCl Ringer's solution. A mean value of V_{bl} was employed ($V_{bl} -52 \pm 1$ mV) which was the mean value of 8 conventional microelectrode readings taken immediately before and after the K^+ -sensitive microelectrode readings (see Table 3). The results gave a mean activity for 10 penetrations in 2 animals of 76 ± 2 mM.

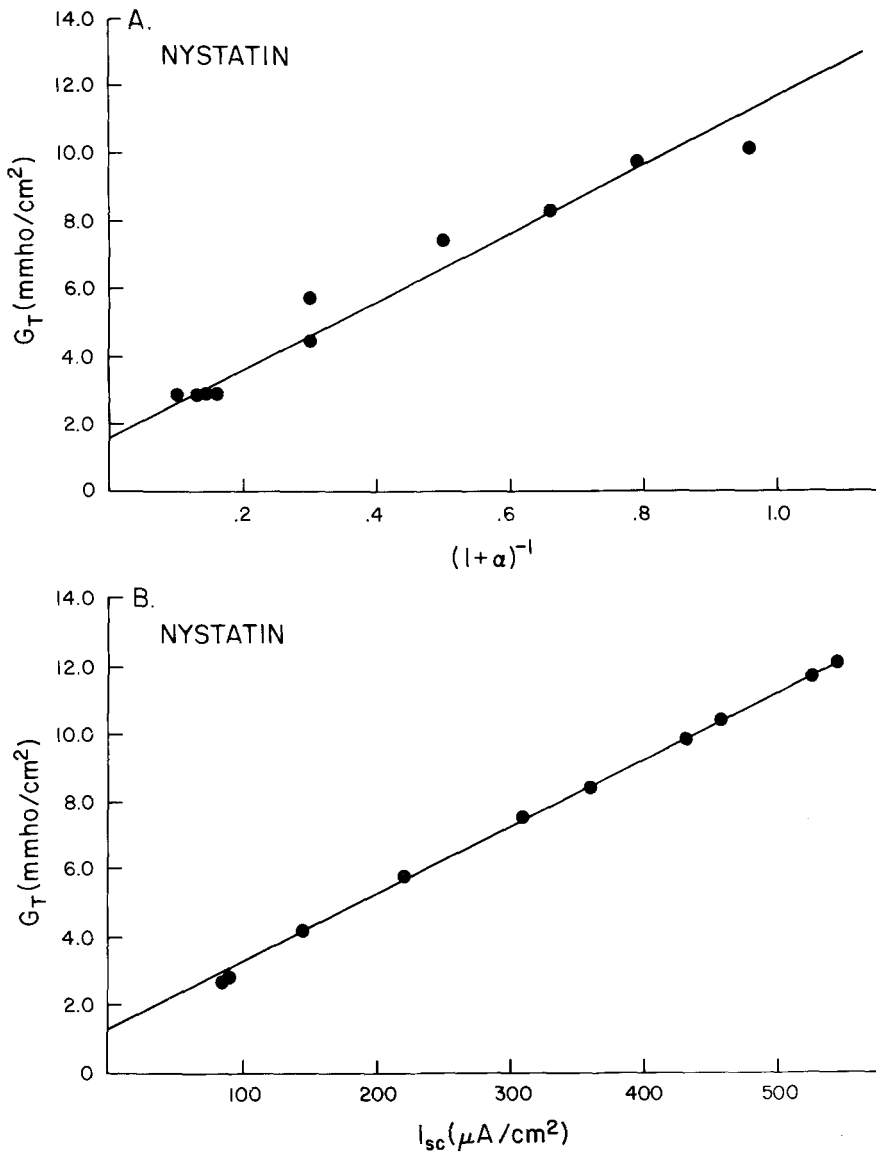


Fig. 3. Comparison of nystatin microelectrode and transepithelial measurements. (A): Nystatin-induced changes in the voltage divider ratio (abscissa) and transepithelial conductance (ordinate) show a linear relationship. The data points are indicated by filled circles, and the straight line shows the results of a linear regression analysis. In this experiment, G_{bl} (slope⁻¹) was 10 mmho/cm² and G_s (zero G_T intercept) was 1.6 mmho/cm². The correlation coefficient was .97. (B): Transepithelial measurements on the same experiment. E_{bl} (slope⁻¹) = 52 mV and G_s (zero G_T intercept) = 1.44 mmho/cm². The correlation coefficient was .99

Table 3. Mean microelectrode measurements of intracellular potassium activity

n	V_i (mV)	V_o^a (mV)	V_{bl} (mV)	$K_{K/Na}$	a_K^o (mM)	a_K^i (mM)
10	12.5	0	-52 ± 1	75/1	5.32	76 ± 2

^a Arbitrarily adjusted to zero.

II. Selective Permeability of the Nystatin-treated Colon. A second step in the identification of the source of the basolateral membrane was to characterize the selective permeability properties of the basolateral membrane to Na^+ , K^+ and Cl^- ions. For this purpose, the apical surface of the colon was bathed with K_2SO_4 Ringer's solution and treated with nystatin, as described previously. After an equilibration period of approximately 5 min, the serosal bathing solution was changed from the normal NaCl Ringer's solution. A sequence of solution changes was performed in which all or part of the serosal Na^+ was replaced by an equimolar amount of K^+ . Under these conditions it is unlikely that a significant potential will arise from electrogenic pump activity, since the mucosal solution contains essentially no Na^+ or Cl^- .

In addition intracellular (K^+) was approximately equal to the mucosal solution potassium (K^+ 78 mM), as measured with K-sensitive liquid ion exchanger microelectrodes.

The measured values of the transepithelial potential (V_T) at each serosal potassium level were then fitted to the following equation (Hodgkin & Katz, 1949) using a nonlinear curve fitting routine on a PDP 11/70 computer in order to estimate selective permeability ratios for sodium (P_{Na}/P_K) and chloride (P_{Cl}/P_K):

$$V_T = \frac{RT}{F} \ln \frac{w}{y} \quad (4)$$

where:

$$w = (K)_s + P_{Na}/P_K (Na)_s + P_{Cl}/P_K (Cl)_m$$

and

$$y = (K)_m + P_{Na}/P_K (Na)_m + P_{Cl}/P_K (Cl)_s.$$

Subscripts m and s refer to the mucosal and serosal solutions, respectively. R , T and F have their usual meaning.

The transepithelial conductance (G_T) was also calculated during the solution changes from the transepithelial voltage response to small, symmetrical current pulses passed across the tissue ($G_T = \Delta I/\Delta V_T$). These results were fitted to the following equation (Hodgkin & Katz, 1949) and solved for P_K (assuming P_{Na}/P_K and P_{Cl}/P_K from Eq. (4) above):

$$G_T = \frac{F^3}{(RT)^2} V_T P_K \cdot \frac{wy}{w-y} \quad (5)$$

where w and y are defined as above.

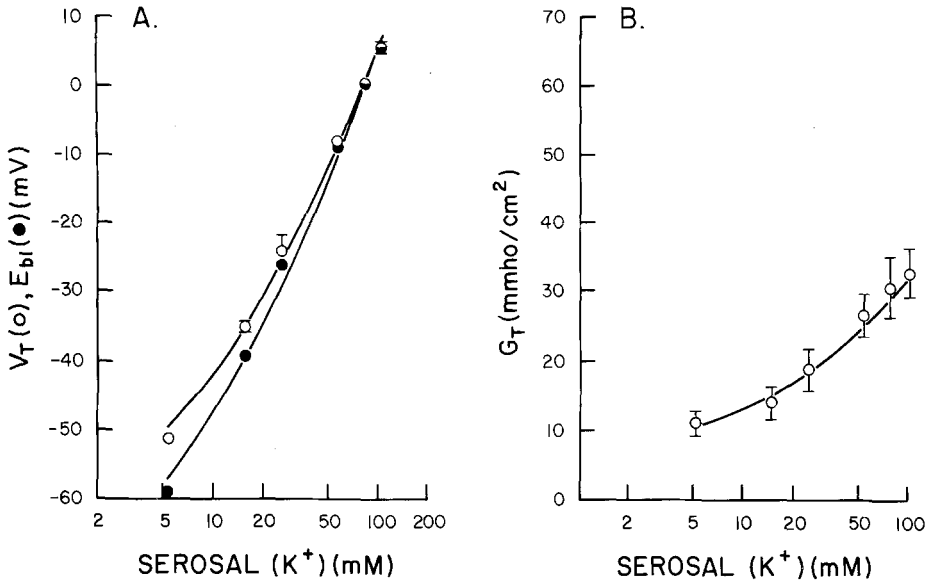


Fig. 4. Selective permeability results: basolateral membrane potential and conductance. (A): Corrected (filled circles) and uncorrected (open circles) values of the basolateral membrane potential as a function of serosal (K^+). To estimate values of P_{Na}/P_K and P_{Cl}/P_K , a nonlinear least squares curve fit of the constant field equation (4) was performed, yielding the following values: uncorrected $P_{Na}/P_K = .08$ and $P_{Cl}/P_K = .07$; corrected $P_{Na}/P_K = .04$ and $P_{Cl}/P_K = .06$ (for details, see text). (B): Mean values of basolateral membrane conductance in nystatin treated colons as a function of serosal K^+ activity. The smooth line is predicted by the constant field Eq. (5). (For description, see text)

P_{Na}/P_K and P_{Cl}/P_K were estimated simultaneously in experiments in which Cl^- was present in the mucosal [10 mM] and serosal [121 mM] bathing solutions.¹ The results of these experiments are shown in Fig. 4a, which presents the transepithelial potential as a function of serosal K^+ activity. The open circles represent mean values from 5 experiments. The smooth curve is the result of a nonlinear curve-fit to Eq. (4). P_{Na}/P_K was estimated as 0.08 and P_{Cl}/P_K was .07.

In a similar analysis the transepithelial conductance was also measured at each serosal K^+ activity. As shown in Fig. 4b, the conductance increased markedly as a function of (K^+). By using the permeability ratios from the transepithelial potential measurements ($P_{Na}/P_K = 0.08$ and $P_{Cl}/P_K = 0.07$) and $P_K = 102 \times 10^{-6}$ (calculated from the lowest conductance value), it was possible to demonstrate that the conductance measurements were well predicted by the constant field equation (Eq. (5)), as shown by the smooth curve.

¹ Initially, we attempted to calculate P_{Na}/P_K and P_{Cl}/P_K independently. Therefore, we first calculated the sodium to potassium permeability ratio under Cl^- -free conditions (sulfate replacement). While the transepithelial voltage results showed a reasonable fit to Eq. (4), the conductance data from the same experiments were not predicted by Eq. (5). Our preliminary calculations indicate that P_K and possibly P_{Na} are decreased as serosal potassium is increased. Similar results have been found for *Sepiolo lens* (Delamere & Duncan, 1977).

The next step in our analysis was to correct for the presence of the shunt pathway, and thus to resolve the selective permeability of the basolateral membrane alone. As previously discussed, we have treated the shunt as a simple nonselective barrier which is in parallel with the basolateral membrane (Fig. 2). The presence of this shunt will attenuate the basolateral membrane emf (E_{bl}). We can correct for this attenuation as follows:

$$E_{bl} = V_T(1 + R_{bl}/R_s). \quad (6)$$

A similar equation was derived by Reuss and Finn (1975) for the *Necturus* gallbladder. Figure 4a (filled circles) illustrates corrected potential values (E_{bl}) at varying serosal (K^+) levels. The smooth curve represents a nonlinear curve fit to the data using Eq. (4) which estimates P_{Na}/P_K at 0.04 and P_{Cl}/P_K at 0.06 for the basolateral membrane alone. We have independently derived the same values for P_{Na}/P_K and P_{Cl}/P_K from the current-voltage relationship of this membrane (S.A. Lewis, D.C. Eaton, N.K. Wills and M. Ifshin, *unpublished*). To calculate the actual permeabilities using Eq. (5), we find for corrected measurements $P_K = 116 \times 10^{-6}$, $P_{Na} = 4.6 \times 10^{-6}$, $P_{Cl} = 7.0 \times 10^{-6}$ cm/sec.

III. Electrogenic Pump. Regardless of whether the basolateral membrane potential is generated by potassium diffusion, a significant potential could still arise from the activity of an electrogenic pump (Carpenter & Alving, 1968). To demonstrate the presence of a pump, nystatin-treated tissues (i.e., $R_a \rightarrow 0$) were bathed on both sides with K_2SO_4 solutions. This procedure caused V_T to depolarize to approximately zero mV. Equal aliquots of NaCl were then added to both serosal and mucosal solutions to yield final concentrations of 8.5, 21.8, 35.1, 48.4 and 61.7 mM. From the total resistance and spontaneous potential values, the short-circuit current was calculated using Ohm's Law. Figure 5 indicates that increases in mucosal (and thus cellular) $[Na^+]$ resulted in a hyperpolarization of the basolateral membrane as reflected by an increase in I_{sc} . Step changes in serosal Na^+ caused negligible changes in V_T and R_T , while mucosal Na^+ addition increased I_{sc} and V_T with stable values occurring within about 2 min. Higher concentrations of NaCl, beyond those shown in Fig. 5, produced negligible changes in I_{sc} or V_T . The increase in V_T averaged 4 ± 1 mV. Inhibition of Na^+K^+ ATPase by serosal addition of ouabain resulted in a rapid (within 80–180 sec) reduction (by 50%) in the potential and current. Similar experiments with KCl addition produced negative results.

Discussion

The results of this study are relevant to two aspects of the colonic epithelial transport: (i) the passive and active transport properties of the basolateral membrane and (ii) the nature of shunt conductance pathway in this tissue.

Source of the Basolateral Membrane Potential

In the following section we will discuss the ionic bases of the basolateral membrane potential as indicated by the selective permeability and active transport properties of this membrane.

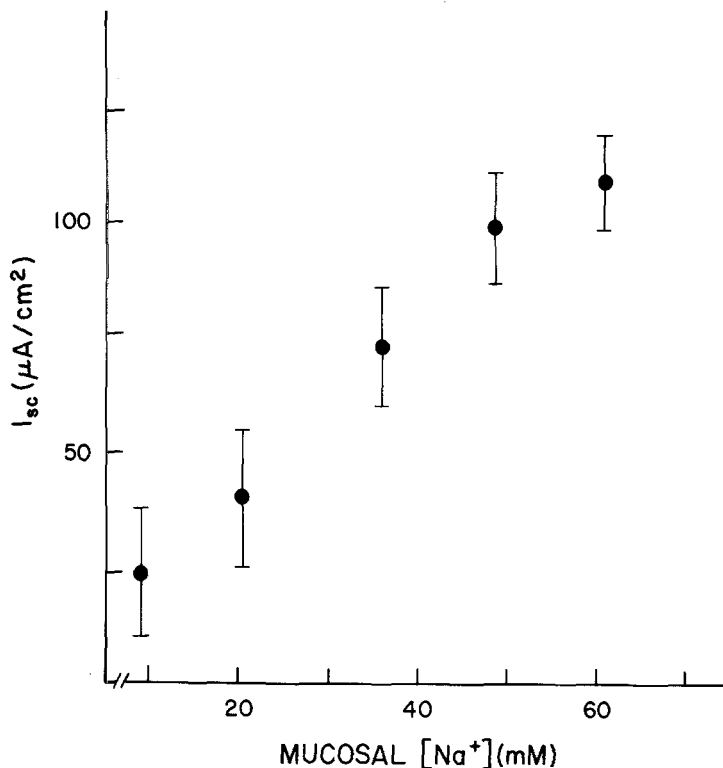


Fig. 5. Change in the short-circuit current (I_{sc}) after stepwise addition of NaCl to mucosal and serosal solutions in a nystatin-treated (apically doped) preparation. The increases in I_{sc} reflect a hyperpolarization of V_T which was rapidly (1-2 min) abolished by serosal addition of ($10^{-4}M$) ouabain

Simultaneously estimated permeability ratios from the constant chloride experiments gave values of $P_{Na}/P_K = .08$ and $P_{Cl}/P_K = .07$, uncorrected for shunt conductance and $P_{Na}/P_K = .04$ and $P_{Cl}/P_K = .06$, for the basolateral membrane alone. The low relative permeability of Na and Cl in comparison to K^+ was not surprising and undoubtedly has physiological significance, as one would anticipate low permeabilities to these ions in a tissue which both actively (and independently) absorbs Na^+ and Cl^- and, in some instances, actively secretes Cl^- (Frizzell *et al.*, 1976; Frizzell, 1977). In view of the high permeability to potassium, the resistance of this membrane (R_{bl}) most probably reflects potassium conductance, G_K .

Our results indicate that while the emf of the basolateral membrane may include an electrogenic component, the primary source of the basolateral membrane potential is passive, since the intracellular (K^+) was too high to be in equilibrium with the resting membrane potential. We calculate the potassium equilibrium potential as -68.3 mV. The nonequilibrium distribution of K^+ across the membrane is probably maintained by an active transport system, presumably a Na^+-K^+ ATPase, which might also be involved in electrogenic transport.

In the present results the activity of the electrogenic Na^+ pump was clearly too small to generate the entire basolateral potential. However, it must be recognized

that the normal functioning of the pump may be altered under the conditions of these experiments. It is difficult to speculate about the physiological function of such a pump. It may be influenced by hormones or respond to increases in intracellular Na^+ to provide some form of "auxillary power" to the normal membrane resting potential. Future experiments should be addressed to the stoichiometry of this pump.

Nature of the Shunt Pathway

Our finding of a close agreement between transepithelial and microelectrode estimates of G_s indicates that the shunt pathway possesses no significant selectivity, at least under the conditions of the nystatin experiments. This finding does not support the view by Frizzell *et al.* (1976) that the paracellular pathway is potassium selective. We note that the original observation reported by Frizzell *et al.* was based on uni-directional transmural fluxes and thus may have neglected the effects of cellular ion gradients. Furthermore, the present calculation of R_j ($770 \Omega\text{cm}^2$) greatly exceeds that reported by Schultz, *et al.* (1977) ($345 \Omega\text{cm}^2$). Thus our results indicate that the colon is a moderately "tight" instead of moderately "leaky" epithelium. While it is conceivable that some aspect of the nystatin experiments may be related to the lack of selectivity and high resistance in the shunt pathway observed in the present experiments, we believe this explanation is unlikely (*see* amiloride results, *Appendix*). Nonetheless, further experiments may be necessary to resolve the issue of whether the junctions are indeed potassium selective under "normal" *in vitro* conditions. A comparison of amiloride and nystatin experiments performed on the same tissues is given in the *Appendix*.

A Common Model

A comparison of our results to the model for Na^+ transport across a tight epithelium presented by Lewis, Eaton and Diamond, 1976 (*see* also Lewis, 1977 and Lewis *et al.*, 1978), indicates a consistent theme. Table 4 compares Na^+ transport phenomena of rabbit urinary bladder and descending colon in terms of I_{sc} and R_T , as well as other parameters.

Under Na^+ transport conditions, the descending colon behaves much like rabbit urinary bladder. Short-circuit current is decreased and total resistance is increased with amiloride and ouabain. Conversely, I_{sc} is increased and R_T decreased with nystatin. A similar influence is exerted by aldosterone on urinary bladder. A difference between the two preparations has been noted in our preliminary experiments which indicate that I_{sc} (not necessarily related to Na^+ transport) and R_T are influenced by neuropharmacologic agents in the colon but not urinary bladder.

A comparison of the membrane properties of the two tissues reveals a high degree of similarity. In general, apical, basolateral, and junctional resistances are higher in urinary bladder, as one would expect from a tissue with relatively low transport rate. Although the selective permeabilities of the apical membrane have

Table 4. Comparison of descending colon and urinary bladder epithelia of the rabbit

Pharmacological agents	Descending colon		Urinary bladder	
	I_{SC}	R_T	I_{SC}	R_T
Amiloride	↓	↑	↓	↑
Ouabain	↓	↑	↓	↑
Aldosterone	↑	↓	↑	↓
Nystatin	↓	↑	↓	↑
Norepinephrine	↓	↓	—	—
Carbachol	↑	↓	—	—
<i>Apical membrane</i>				
Permeability	Na ⁺ (Cl ⁻ ?)		(Na ⁺)	
Negative feedback	yes		yes	
Resistance	~700 Ωcm ²		5,000–100,000 Ωcm ²	
<i>Basolateral membrane</i>				
P_{Na}/P_K	.04		.05	
P_{Cl}/P_K	.06		1.17	
Resistance	95 Ωcm ²		1500 Ωcm ²	
Potential	K ⁺ diffusion		K ⁺ diffusion	
Ouabain sensitive	yes		yes	
Electrogenic pump	yes		yes	
<i>Tight Junction</i>	730 Ωcm ²		>300,000 Ωcm ²	

not yet been assessed, some evidence (Schultz *et al.*, 1977) indicates that the membrane is primarily Na⁺ selective. However, if our analysis is correct, the membrane also has a leak conductance (*see Appendix*). In addition, Lewis *et al.* (1976) found evidence that apical membrane conductance was decreased with high intracellular [Na⁺], a phenomenon similar to the transinhibition reported by Turnheim, Frizzell and Schultz (1977) for colon.

With respect to the source of basolateral membrane potential, both tissues appear to behave essentially as K⁺ electrodes, although an electrogenic, ouabain-sensitive pump may be present. Both epithelia show relatively low basolateral membrane permeabilities to Na⁺, $P_{Na}/P_K = .04$ for both colon and bladder. However, they are different with respect to P_{Cl}/P_K . Urinary bladder is quite permeable to Cl⁻ ($P_{Cl}/P_K = 1.17$), but colon is relatively impermeable ($P_{Cl}/P_K = .06$). Possibly this difference is related to the ability of the colon to secrete Cl⁻ under certain hormonally induced conditions.

In conclusion, Na⁺ transport across descending colon is highly similar to Na⁺ transport across the tight epithelium rabbit urinary bladder, although the membrane and junctional resistances of colon are significantly lower. This similarity indicates that Na⁺ transport in tight and "moderately" tight epithelia may be accomplished by a common mechanism. Furthermore, by investigating alterations in transport within the framework of such a model, it may be possible to further elucidate the nature of colonic epithelial transport.

This work was supported by N.I.H. grant AM 20851 to S.A. Lewis and AM 20068 and AM 00432 to D.C. Eaton.

Appendix

The Effects of Amiloride on the Electrical Properties of the Colon and an Equivalent Circuit Model

The purpose of the present amiloride experiments was to obtain additional information concerning the electrical properties of the colon in the same tissues which were studied in the preceding report. By comparing amiloride and nystatin-derived estimates of shunt and membrane resistances and cellular emf's, it was possible to develop a comprehensive model of colonic transport which includes the presence of a leak ion pathway in the apical membrane and incorporates heterogeneous cell types. We will first describe the effects of amiloride and the method for calculation of membrane parameters from these results.

The procedures for the amiloride studies were essentially identical to the nystatin experiments described earlier except that NaCl Ringer's was the mucosal solution. As summarized in Table 5, the addition of 1×10^{-4} amiloride to the mucosal side produced a sharp decrease in V_T and I_{sc} . The rate of this reaction was related to the stirring of the bathing solution but usually occurred within 20 sec. Concurrently, V_{bl} hyperpolarized slightly and R_T and α ($\alpha \equiv R_a/R_{bl}$) increased. Similar results have been reported by Schultz *et al.* (1977).

As with the nystatin experiments, membrane parameters were estimated from both microelectrode and transepithelial measurements. We will first describe the transepithelial results. Two parameters were estimated: the transepithelial emf and shunt conductance. To estimate these values we used the technique initiated by Yonath and Civan (1971) and employed more recently by Issacson (1977) and Fieg, Wetzel and Frazier (1977) on toad urinary bladder. The basis of this method is derived from the equivalent circuit (given in Fig. 6). In brief, the Na^+ transport pathway is modeled as a battery E_{Na} (the transepithelial emf) in series with a resistor R_{Na} (the resistive pathway for sodium). This series combination is in parallel with a shunt resistance, R_s (nominally assumed to be the junctional resistance). Thus the transepithelial potential can be described as:

$$V_T = \frac{E_{\text{Na}} G_{\text{Na}}}{G_{\text{Na}} + G_s} \quad (\text{A1})$$

The short circuit current is $I_{sc} = E_{\text{Na}} G_{\text{Na}}$ and total conductance is $G_T = G_{\text{Na}} + G_s$. Substituting for G_{Na} , $G_T = 1/E_{\text{Na}} (I_{sc}) + G_s$. Thus a plot of G_T vs. I_{sc} will have an inverse slope of E_{Na} (on the assumption that the only parameter changing in the equivalent circuit is R_{Na}), and zero conductance G_T intercept equal to G_s .

The equivalent circuit described above makes no distinction between the role of apical and basolateral cell membranes in epithelial Na^+ transport. An equivalent circuit which models the two membranes is presented in Fig. 7 (see also Schultz *et al.*, 1977). In this circuit, E_a^{Na} is the sodium battery in the apical membrane and R_a^{Na} its resistance. R_{bl} and E_{bl} are the resistance and emf of the basolateral membrane, and R_s is the shunt resistance. In terms of this circuit:

$$G_T = (E_a^{\text{Na}} + E_{bl})^{-1} (I_{sc}) + G_s \quad (\text{A2})$$

Assuming that I_{sc} is completely accounted for by Na^+ transport and that experi-

Table 5. Amiloride microelectrode results

	V_T (mV)	R_T (Ωcm^2)	V_{bl} (mV)	α	Estimated resistance (Ωcm^2)		
					R_a	R_{bl}	R_s
Control (NaCl mucosal and serosal solution)	-21 ± 6	282 ± 29	-52 ± 1	4 ± 1	644 ± 225	161 ± 31	498 ± 70
Amiloride (10^{-4} M mucosal solution $n = 5$)	0 ± 3^b	360 ± 50^a	-54 ± 1^a	10 ± 3^a	$1,610 \pm 439$	---	---

^a $P < .05$.^b $P < .01$.

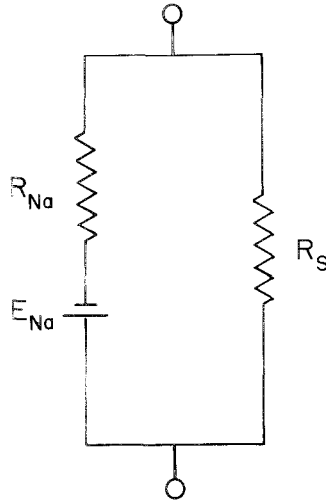


Fig. 6. A simplified equivalent circuit for Na^+ transport. R_{Na} and R_s represent sodium and shunt resistances, respectively. E_{Na} is the Na^+ driving force

mental manipulations alter only G_a^{Na} , the sodium driving force and shunt conductances from the earlier model become:

$$E_{\text{Na}} = \text{Slope}^{-1} = (E_a^{\text{Na}} + E_{bl}) \quad (\text{A3})$$

and G_s equals the zero conductance intercept.

By assuming that amiloride selectively decreases G_a^{Na} (Ussing, Erlj & Lassen, 1974), we found that the mean value for E_{Na} (or Slope^{-1}) was 120 ± 11 mV ($n = 5$;

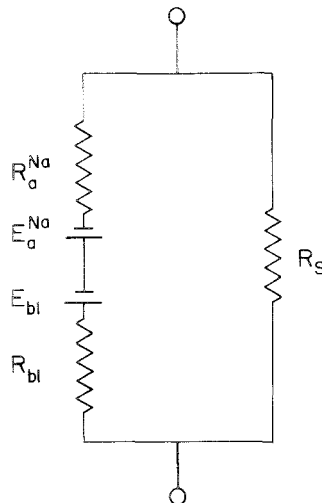


Fig. 7. Two-membrane equivalent circuit model of Na^+ transport. R_a^{Na} and R_{bl} are the resistances of the apical and basolateral membranes; E_a^{Na} and E_{bl} are their respective emf's. R_s is shunt resistance

see Eq. (A3)) and the inverse intercept (R_s) equalled $380 \pm 60 \Omega\text{cm}^2$. A representative experiment is shown in Fig. 8.

As in nystatin experiments, shunt resistance can also be estimated from microelectrode measurements. However, in amiloride experiments, we found it more convenient to use the method of simultaneous equations (Lewis *et al.*, 1976) as follows:

$$\begin{aligned} G_T &= G_s + G_{bt}(1 + \alpha)^{-1} \\ G'_T &= G_s + G_{bt}(1 + \alpha')^{-1} \end{aligned} \quad (\text{A4})$$

where G_T , G'_T , α and α' are the transepithelial conductance and voltage divider ratios before and after mucosally applied amiloride, respectively. G_s and G_{bt} are assumed to be independent of mucosal amiloride as found by Lewis *et al.* (1976), Lewis (1977), Lewis *et al.* (1977) and Schultz *et al.* (1977).

The two equations are then solved for $R_s(1/G_s)$ and $R_{bt}(1/G_{bt})$. R_a was calculated as $\alpha \cdot G_{bt}$, and $R'_a = \alpha' G_{bt}$. Mean values from 5 experiments were $R_a = 644 \pm 225 \Omega\text{cm}^2$, $R'_a = 1,610 \pm 439 \Omega\text{cm}^2$, $R_{bt} = 161 \pm 31 \Omega\text{cm}^2$ and $R_s = 498 \pm 70 \Omega\text{cm}^2$. Note that this R_s value disagrees with the preceding transepithelial measurements of R_s ($380 \Omega\text{cm}^2$) ($t = -4.10$; $df = 4$; $p < .01$).

A second striking difference which emerged from the analysis of the amiloride experiments was the disagreement between amiloride and nystatin microelectrode estimates of shunt resistance from the same tissues (t for paired means = 3.66; $df = 3$, $p < .025$). The significance of these differences in R_s will be examined in the following discussion.

I. Disagreement Between Transepithelial and Microelectrode Estimates of R_s

As noted above, the "transepithelial" and microelectrode estimates of shunt resistance from amiloride experiments were significantly different (see Table 5). However, it should be noted that the transepithelial measurement of shunt resis-

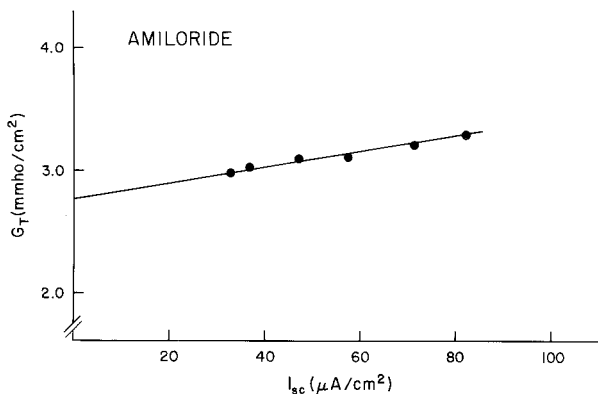


Fig. 8. Amiloride transepithelial measurements. A representative amiloride experiment. Linear regression analysis provided the following values for E_{Na} : (slope⁻¹) = 164.6 mV and G_s (G_T intercept) = 2.74 mmho/cm² ($r = .96$)

tance is in good agreement with that reported by Schultz *et al.* (1977). Thus our microelectrode estimate differs both with the transepithelial estimate and previously reported values. It is doubtful that impalement damage is responsible for the discrepancy between our microelectrode results and Schultz *et al.* (1977) because such an artifact would cause both an overestimate of junctional resistance and underestimate of basolateral resistance, and our estimate of basolateral membrane resistance from amiloride experiments is higher than that reported by these authors. A more likely explanation for this discrepancy follows from the assumption in transepithelial measurements that the apical membrane is permeable to only Na⁺ (see Figs. 6 and 7). Thus any leak resistance in the apical membrane from transepithelial measures will be lumped into the shunt resistance term as indicated in the equivalent circuit in Fig. 9. The value of the apical membrane leak resistance can, therefore, be calculated as the difference of the transepithelial and microelectrode shunt resistance estimates minus the basolateral resistance. The minimum value for leak resistance calculated in this manner is 1600 ohm cm².

A parallel leak battery in the apical membrane can be determined as follows. Cellular emf (E_c) was calculated from the relationship

$$E_c = \frac{V_T}{R_T} \cdot R_c \tag{A5}$$

where R_c is the cellular resistance determined using microelectrodes and

$$R_c = R_a + R_{bl} \text{ where } R_a = \frac{R_a^{Na} R_a^L}{R_a^{Na} + R_a^L}$$

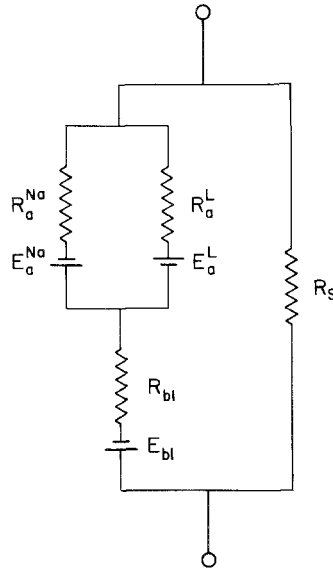


Fig. 9. Revised “two-membrane” equivalent circuit model. The circuit is essentially identical to Fig. 7 except that a leak resistance and battery (R_a^L and E_a^L) are placed in parallel with the Na⁺ pathway in the apical membrane

In terms of this circuit E_c is equal to

$$E_c = \left(\frac{E_a^{Na}}{R_a^{Na}} + \frac{E_a^L}{R_a^L} \right) R_a + E_{bl}. \quad (\text{A6})$$

I_{sc} was calculated as V_T/R_T or E_c/R_c from our amiloride data. A value of E_a^L was then determined from the best fit to a plot of E_c vs. I_{sc} (Fig. 10). The values used for E_a^{Na} , E_{bl} , R_{bl} and R_a^L were 60 mV, 57 mV, 160 Ωcm^2 and 1600 Ωcm^2 . R_a^{Na} was varied from 10,000 to 500 Ωcm^2 . The best fit E_a^L was 57 mV (cell interior negative). Such a potential indicates that the measured I_{sc} will be equal to the net Na flux. In addition, complete inhibition of Na^+ transport will result in a zero transepithelial potential. Possible candidates for the leak resistance and emf are H^+ , K^+ or Cl^- .

Perhaps the most interesting feature of such a model is that it allows a single cell to possess more than one transport system. As an example, the colon is known to secrete Cl^- under certain physiological conditions. If this leak resistance is indeed a Cl^- selective pathway, then by regulating intracellular (Cl^-) through a basolateral Cl^- pump the electrochemical gradient could be altered so that Cl^- is either secreted or reabsorbed across the apical membrane.

II. Disagreement with Nystatin Estimates of R_s

A second statistically significant difference in our results emerged between the amiloride and the nystatin estimates of R_s . This difference could potentially be explained by several hypotheses: (i) Perhaps the tight junctions are more permeable to Cl^- than SO_4^{2-} . Therefore, replacement of NaCl by K_2SO_4 would result in a relative increase in R_s ; (ii) maybe nystatin alters the size of the lateral intercellular spaces (LIS), thus changing the estimate of R_s , and (iii) perhaps not all cells in the colon are affected by amiloride.

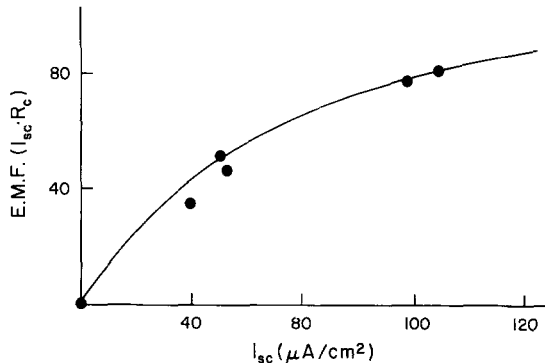


Fig. 10. Calculated cellular emf (text, Eq. (5)) as a function of I_{sc} . The solid line is a best fit of Eq. (6) to the data, yielding an E_a^L value of 54 mV (cell interior negative). For details, see text

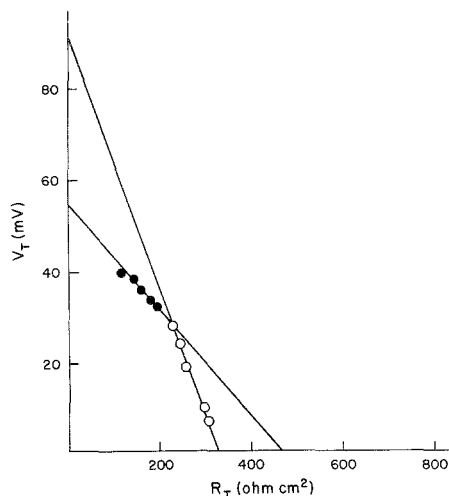


Fig. 11. The results of separate nystatin (filled circles) and amiloride (open circles) experiments on the same tissue. In the amiloride experiment, Cl^- was replaced with SO_4^{-2} . NaSO_4 experiments are represented as V_T vs. R_T . The V_T intercepts of the amiloride and nystatin experiments represent E_{Na} and E_{bb} , respectively, and the R_T intercept is shunt resistance. Note that under these conditions nystatin estimates of R_s remain larger than amiloride values

To test the first hypothesis, we replaced the mucosal Cl^- with SO_4^{-2} , assuming that Na^+ and K^+ are equally permeable through the tight junctions. We then re-estimated R_s using amiloride techniques and nystatin on the same preparation. A comparison of the data is given in Fig. 11. This data is plotted as V_T vs. R_T , thus R_s for each experiment is represented by the zero voltage intercept², R_{T_i} . As can easily be seen in this diagram, R_s for the amiloride experiment (open circles) is smaller than R_s as determined by the nystatin experiment (filled circles). Consequently, we conclude that the use of different solutions probably does not account for the discrepancy between nystatin and amiloride estimates, although further study would be desirable to more conclusively answer this question.

It is similarly doubtful that the second hypothesis, that nystatin causes the lat-

² A plot of V_T vs. R_T yields the same information as G_T vs. I_{sc} . It offers the following advantages: (i) the preparation does not have to be continuously short circuited and (ii) the x intercept yields R_s and the y intercept E_{Na} , eliminating the need to interpret the value of the inverse slope. The derivation is straight-forward. Using Fig. 13, one can express total resistance in terms of the individual resistors, $1/R_T = 1/R_s + 1/R_{\text{Na}}$. Multiplying by R_T and substituting V_T/E_{Na} for R_T/R_{Na}

$$\left(V_T = \frac{E_{\text{Na}}}{R_{\text{Na}}} \cdot R_T \right)$$

we have a 2 intercept linear equation $1 = V_T/E_{\text{Na}} + R_T/R_s$ on the assumption that any manipulation alters only R_{Na} .

eral intercellular spaces (LIS) to swell or collapse, can explain the data. Because the exposed area of the basolateral membrane is negatively correlated with the size of LIS, any changes in junctional and basolateral conductance should occur in the same direction. However, comparison of nystatin and amiloride experiments do not demonstrate this relationship: nystatin estimates of G_s (or R_s^{-1}) are smaller than amiloride estimates while G_{bl} (or R_{bl}^{-1}) estimates are larger. Consequently, an adequate explanation of the disparity between amiloride measures must not only explain differences in junctional conductance estimates but should also account for the discrepancy between cellular membrane conductance estimates.

With respect to the third hypothesis, it is plausible that some cells in the colon may be insensitive to amiloride, but the present equivalent circuit does not permit us to postulate how the presence of a heterogeneous cell population would influence amiloride estimates of G_s . A revision of the circuit which takes into account the effects of different cell types is presented below. The strength of this hypothesis, as will be shown below, is that the inclusion of amiloride-insensitive cell types can account for discrepancies between amiloride and nystatin estimates of R_s . Furthermore, it predicts differences in the estimates of cell membrane conductances, G_a and G_{bl} .

Revised Equivalent Circuit

The proposed revision of the equivalent circuit model of the colon is shown in Fig. 12. In this circuit, E_a^{Na} and E_a^L are the sodium and leak batteries in the apical membrane of the amiloride sensitive cells. R_c (R_a^c and R_b^c) is the resistance of a nontransporting cell type in which the batteries of the apical and basolateral membrane are equal and opposite in polarity, thus contributing no net emf to the transepithelial potential. (This assumption is supported by the finding of Schultz *et al.* (1977) that I_{sc} is equal to net Na^+ transport.) The circuit assumes:

- 1) All potentials are caused by ionic gradients; i.e., are diffusion potentials.
- 2) Since I_{sc} is entirely accounted for by sodium transport, $E_a^L + E_{bl} = 0$.³
- 3) There are no batteries in series with the junctional resistance.

The above three assumptions are equivalent to the single assumption that all cell types are coupled by zero resistance pathways. To simplify the following discussion we will refer to all resistances in terms of their corresponding conductances (e.g., $G_s = R_s^{-1}$).

Experiments performed using nystatin and measuring the change in α , as well as I_{sc} , will yield the following terms: from microelectrode experiments a plot of G_T vs. $(1 + \alpha)^{-1}$ will have a slope = $G_{bl} + G_{bl}^c$ and an intercept of $G_s = G_j$. From transepithelial measurements a plot of G_T vs. I_{sc} will have an intercept of $G_s = G_j$ and

³ We can imagine the situation where the so-called nontransporting cells have a potential equal and opposite to that of the amiloride inhibited cells; i.e.,

$$\frac{E_a^L - E_{bl}}{R_a^L + R_{bl}} = - \frac{E_c}{R_c}$$

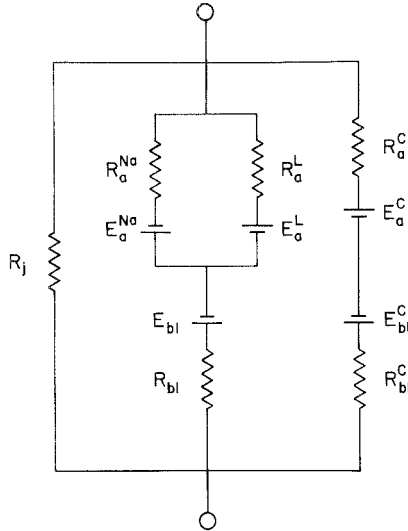


Fig. 12. Proposed equivalent circuit of the colon revised to include amiloride insensitive cells types. R_a^c and R_{bl}^c represent the apical and basolateral membrane resistances. E_a^c and E_{bl}^c are the apical and basolateral emf's of these cells. For description, see text

an inverse slope of

$$\frac{E_{bl} R_{bl}^c + E_{bl}^c R_{bl}}{R_{bl} + R_{bl}}$$

(see assumption 2). Thus,

$$G_T = \frac{I_{sc}}{E_{bl}} + G_j .$$

Note that under the conditions ($E_a^{Na} = E_a^L = E_a^c = 0$), I_{sc} is not necessarily related to Na^+ transport.

Significance of G_j : We now return to our earlier hypothesis concerning the discrepancy between amiloride and nystatin estimates of G_s . Perhaps the most obvious feature of the above analysis is that G_s , as derived for amiloride experiments, has a different value than G_s derived for nystatin experiments. The difference between the two terms is the inclusion of amiloride-insensitive cell conductances in amiloride estimates of G_s . Consequently, according to our equations, G_s will be overestimated by amiloride techniques and will equal tight junctional conductance as measured by nystatin methods.

If indeed the difference between amiloride and nystatin estimates of junctional resistance is due to the presence of heterogeneous cell types, then by subtracting G_j from G_s , it is possible to calculate the conductance of the amiloride insensitive cells. Performing such an operation, we find the conductance of these cells is equal to 0.56 mmho/cm². Assuming amiloride sensitive and insensitive cells were of equal volume (and resistance) then the distribution of amiloride sensitive to insensitive cells would be approximately 3:1.

Significance of G_a and G_{bl} : As previously indicated, amiloride and nystatin techniques also differed concerning the resolution of cellular conductance into its membrane components, G_a and G_{bl} . As with G_s estimates it is likely that this discrepancy arises from respective differences in the meaning of shunt conductances. Because G_{bl} and G_a estimates are calculated from G_s (see Eq. (1), *Methods*), these estimates will similarly differ such that amiloride estimates of G_a and G_{bl} represent only amiloride-sensitive cells while nystatin measures of G_a and G_{bl} provide average terms for all cell types. It should be noted that until the total surface area of each cell type is known, it is not possible to convert the amiloride conductance estimates to actual resistance values.

In summary, we have found statistically significant differences between amiloride transepithelial and microelectrode estimates of shunt resistance which are consistent with a finite leak conductance in the apical membrane. Similar differences between amiloride and nystatin estimates of R_s , may make it possible to resolve the conductances of amiloride sensitive and insensitive cell types in the colon.

References

- Carpenter, D.O., Alving, B. 1968. A contribution of an electrogenic Na^+ pump in membrane potential of *Aplysia* neurons. *J. Gen. Physiol.* **52**:1
- Cass, A., Dalmark, M. 1973. Equilibrium dialysis of ions in nystatin-treated red cells. *Nature New Biol.* **244**:47
- Cass, A., Finkelstein, A., Krespi, V. 1970. The ion permeability induced in thin lipid membranes by polyene antibiotics nystatin and amphotericin B. *J. Gen. Physiol.* **50**:100
- Delamere, N.A., Duncan, G. 1977. A comparison of ion concentrations, potentials and conductances of amphibian, bovine and cephalopod lenses. *J. Physiol. (London)* **272**:167
- Feig, P.U., Wetzel, G.D., Frazier, H.S. 1977. Dependence of the driving force of the sodium pump on rate of transport. *Am. J. Physiol.* **232**:F448
- Frizzell, R.A. 1977. Active chloride secretion by rabbit colon: Calcium-dependent stimulation by ionophore A23187. *J. Membrane Biol.* **35**:175
- Frizzell, R.A., Koch, M.J., Schultz, S.G. 1976. Ion transport by rabbit colon. I. Active and passive components. *J. Membrane Biol.* **27**:297
- Frizzell, R.A., Turnheim, K. 1978. Ion transport by rabbit colon. II. Unidirectional sodium influx and the effects of amphotericin B and amiloride. *J. Membrane Biol.* **40**:193
- Hodgkin, A., Katz, B. 1949. The effect of sodium ions on the electrical activity of the giant axon of the squid. *J. Physiol. (London)* **108**:37
- Holz, R., Finkelstein, A. 1970. The water and electrolyte permeability induced in the lipid membrane by the polyene antibiotics nystatin and amphotericin B. *J. Gen. Physiol.* **56**:125
- Isaacson, L.C. 1977. Resolution of parameters in the equivalent circuit of the sodium transport mechanism across toad skin. *J. Membrane Biol.* **30**:301
- Lewis, S.A. 1977. A reinvestigation of the function of the mammalian urinary bladder. *Am. J. Physiol.* **232**(3):F187
- Lewis, S.A., Diamond, J.M. 1976. Na^+ transport by rabbit urinary bladder, a tight epithelium. *J. Membrane Biol.* **28**:1
- Lewis, S.A., Eaton, D.C., Clausen, C., Diamond, J.M. 1977. Nystatin as a probe for investigating the electrical properties of a tight epithelium. *J. Gen. Physiol.* **70**:427

- Lewis, S.A., Eaton, D.C., Diamond, J.M. 1976. The mechanism of Na⁺ transport by rabbit urinary bladder. *J. Membrane Biol.* **28**:41
- Lewis, S.A., Wills, N.K., Eaton, D.C. 1978. Basolateral membrane potential of a tight epithelium: Ionic diffusion and electrogenic pumps. *J. Membrane Biol.* **41**:117
- Reuss, L. 1978. Mechanism of transepithelial hyperpolarization produced by amphotericin B in *Necturus* gall bladder. *Biophys. J.* **21**:168a
- Reuss, L., Finn, A.L. 1975. Electrical properties of the cellular transepithelial pathway in *Necturus* gallbladder. II. Ionic permeability of the apical cell membrane. *J. Membrane Biol.* **25**:141
- Russell, J.M., Eaton, D.C., Brodwick, M.S. 1977. Effects of nystatin on membrane conductance and internal ion activities in *Aplysia* neurons. *J. Membrane Biol.* **37**:137
- Schultz, S.G., Frizzell, R.A., Nellans, H.N. 1977. Active sodium transport and the electrophysiology of rabbit colon. *J. Membrane Biol.* **33**:351
- Spennney, J.G., Shoemaker, R.L., Sachs, G. 1974. Microelectrode studies of fundic gastric mucosa: Cellular coupling and shunt conductance. *J. Membrane Biol.* **19**:105.
- Turnheim, K., Frizzell, R.A., Schultz, S.G. 1977. Effects of anions on amiloride-sensitive, active sodium transport across rabbit colon, *in vitro*. *J. Membrane Biol.* **37**:63
- Ussing, H.H., Erlj, D., Lassen, U. 1974. Transport pathways in biological membranes. *Annu. Rev. Physiol.* **36**:14
- Yonath, J., Civan, N.M. 1971. Determination of the driving force of the Na⁺ pump in toad bladder by means of vasopressin. *J. Membrane Biol.* **5**:366